Continental Shelf Research 153 (2018) 75–85

Contents lists available at ScienceDirect

Continental Shelf Research

journal homepage: www.elsevier.com/locate/csr

Spatio-temporal variation in $\delta^{13}C_{DIC}$ of a tropical eutrophic estuary (Cochin estuary, India) and adjacent Arabian Sea

P.S. Bhavya[a,1], Sanjeev Kumar[a,*], G.V.M. Gupta[b], K.V. Sudharma[b], V. Sudheesh[b]

[a] Physical Research Laboratory, Ahmedabad 380009, India
[b] Centre for Marine Living Resources and Ecology, Ministry of Earth Sciences, Kendriya Bhavan, Cochin 682037, India

ARTICLE INFO

Keywords:
Carbon
Isotopes
Estuarine
Coastal
Processes

ABSTRACT

Carbon isotopic composition of dissolved inorganic carbon ($\delta^{13}C_{DIC}$) in the Cochin estuary, a tropical eutrophic estuary along the southwest coast of India, and the adjacent coastal Arabian Sea was measured to understand spatio-temporal variability in sources and processes controlling inorganic carbon (C) dynamics in this estuarine-coastal system. $\delta^{13}C_{DIC}$ in the Cochin estuary showed wide variation during three different seasons (premonsoon: − 12.2 to − 3.26‰; monsoon: − 13.6 to − 5.69‰; and postmonsoon: − 6.34 to + 0.79‰). Detailed mixing curve approximation modeling along with relationships of $\delta^{13}C_{DIC}$ with dissolved oxygen and nutrients suggest dominant role of freshwater mixing and degassing of CO_2 on DIC dynamics during wet seasons (premonsoon and monsoon). Excess CO_2 brought in by rivers and in situ production due to respiration in the Cochin estuary result into one of the highest pCO_2 observed in estuarine systems, leading to its degassing. During postmonsoon, a relatively dry period with high salinity, calcite precipitation was a major process with calcite saturation index > 1 at few locations. Relatively lower average surface values of $\delta^{13}C_{DIC}$ in the coastal Arabian Sea (premonsoon: + 0.95‰; monsoon: + 0.88‰; and postmonsoon: + 0.66‰) compared to the predicted open ocean value along with mixing curve modeling suggest dominance of respiration/organic matter (OM) degradation over primary productivity. Estuarine influence on coastal DIC dynamics was observed in nearshore region (~ 10 km), whereas evidence of upwelling was found at farther locations.

1. Introduction

In aquatic ecosystems, carbon (C) isotopic composition of dissolved inorganic carbon ($\delta^{13}C_{DIC}$) can provide information about its sources and sinks, and in turn, the role of anthropogenic and natural inputs in our ecosystems (Degens et al., 1969). Different biogeochemical processes also potentially alter the inputs and outputs of dissolved inorganic carbon (DIC) in an aquatic ecosystem (Oana and Deevey, 1960). DIC inputs to an ecosystem can be through diffusion of atmospheric CO_2, organic respiration, surface runoff, groundwater inflow, calcite dissolution, and methane oxidation. The removal of DIC includes evasion of CO_2, calcite precipitation, photosynthetic uptake, and water outflow. The preference for ^{12}C during bacterioplankton assimilation and degassing of CO_2 results into ^{13}C enriched DIC pool. During respiration/organic matter (OM) degradation, however, CO_2 derived is depleted in ^{13}C, thereby introducing a C pool depleted in ^{13}C into the aqueous medium. Therefore, higher primary productivity and degassing of CO_2 results in higher $\delta^{13}C_{DIC}$, whereas higher rates of decomposition of biota lowers the $\delta^{13}C_{DIC}$ (Mook and Tan, 1991).

In the coastal ocean, surface $\delta^{13}C_{DIC}$ distribution is specifically controlled by air-sea CO_2 exchange, biological productivity, vertical mixing, and sea surface temperature. The bottom waters along the continental shelf, however, are mostly influenced by community respiration and OM degradation. The determination of long-term changes in $\delta^{13}C_{DIC}$ is difficult due to the paucity of data (Quay et al., 1992, 2003; Sonnerup et al., 2000). In general, $\delta^{13}C_{DIC}$ of surface ocean water ranges from 0 to 2‰ whereas values in deeper waters below the mixed layer are around + 0.5 ± 0.5‰ (Mook and Tan, 1991). DIC in the surface waters is expected to be enriched in ^{13}C due to removal of isotopically light C during primary production (Mook, 1970). The relative dominance of different processes varies depending on the region and season (Racapé et al., 2010). In addition to the atmospheric influence, the exchange between the terrestrial and marine C pools also play an important role in controlling the oceanic $\delta^{13}C_{DIC}$ (Broecker and Peng, 1993; Keir, 1998), particularly estuarine and ground water effluents.

Limited studies have been conducted vis-à-vis $\delta^{13}C_{DIC}$ in the tropical regions, especially in India, to understand the C dynamics of

* Corresponding author.
E-mail addresses: bhavya5@pusan.ac.kr (P.S. Bhavya), sanjeev@prl.res.in (S. Kumar).
[1] Now at: Pusan National University, Busan, South Korea.

https://doi.org/10.1016/j.csr.2017.12.006
Received 18 February 2017; Received in revised form 30 October 2017; Accepted 9 December 2017
Available online 15 December 2017
0278-4343/

ecologically important estuary-coastal coupled systems. Based on $\delta^{13}C_{DIC}$ profiles, Godavari estuary in the eastern India has been characterized with carbonate dissolution as an important process determining the DIC dynamics and mangrove creeks as active sites of mineralization (Bouillon et al., 2003). Anthropogenically dominated Hooghly estuary in the eastern India is recorded with low/high $\delta^{13}C_{DIC}$ towards the end of monsoon/premonsoon due to low/high productivity (Ghosh et al., 2013) while its biological respiration together with organic carbon degradation dominated over the biological production (Samanta et al., 2015).

Majority of Indian estuaries studied with respect to DIC dynamics are located on the east coast of India as major Indian rivers drain into the Bay of Bengal. The estuaries on the west coast have not received due attention so far in this regard. The most prominent among them is the Cochin estuary, the longest Indian estuary along the west coast of India. The Cochin estuary is an eutrophic estuary, which receives effluents from many industries, aquaculture ponds and fields leading to biogeochemical imbalance with respect to C and nitrogen (N) cycling (Gupta et al., 2009; Martin et al., 2013). The organic matter loading from the terrestrial ecosystems into the estuary leads to C excess resulting into CO_2 supersaturation and degassing (Gupta et al., 2009). Recent C isotopic studies in this estuary showed distinct zonal pattern with different dominant processes i.e., northern estuary by mixing of seawater and southern estuary and Vembanad Lake by terrestrial inputs (Bhavya et al., 2016a). The high C and N uptake rates in this estuary resulted in less export potential to affect mainly the nearshore coastal biogeochemistry (Bhavya et al., 2016b, 2017). Given its dynamic nature, it is important to investigate the fate of inorganic and organic C and major processes controlling the DIC dynamics in the Cochin estuary.

In view of the above, the present study attempted to decipher sources and pathways of DIC in the Cochin estuary and the adjacent coastal Arabian Sea during three different seasons. The major objectives of the study were to (1) understand the factors influencing C cycling in the Cochin estuary and the coastal Arabian Sea by using $\delta^{13}C_{DIC}$ as a proxy, (2) characterize the seasonal variations in $\delta^{13}C_{DIC}$ of the estuarine-coastal coupled systems, (3) determine whether the coastal Arabian Sea is a source or sink of CO_2, and (4) test for the presence or absence of signatures of the oceanic Suess effect in the coastal Arabian Sea.

2. Materials and methods

2.1. Study area

2.1.1. Cochin estuary

Cochin estuary is a eutrophic micro-tidal system (Fig. 1a) with two openings to the Arabian Sea (Barmouth (station 3) and Azhikode) through which saline water and nutrients are exchanged. Total annual freshwater input from various sources to this estuary is about 20,000 Mm^3, making it the largest wetland along the west coast of India (Srinivas et al., 2003). Freshwater inputs from three major rivers, six main canals and tidal influence from the Arabian Sea regulate the salinity in the estuary with near zero during monsoon and a gradual salinity gradient (34–13) during pre- and postmonsoon (Madhupratap, 1987). The effect of freshwater and tidal cycle on DIC dynamics is not well known in this estuary.

The sampling in the Cochin estuary was performed during April (premonsoon), September (monsoon), and December (postmonsoon) of the year 2012. Surface water samples were collected from seven stations (five across the salinity gradient in the estuary (Station 1–5) and two in the freshwater Vembanad Lake (Stations 6a and 6b; Fig. 1a)). During postmonsoon, however, surface samples were collected from eighteen locations, including five regular stations (except 2 and 6b) mentioned above (Fig. 1b; Bhavya et al., 2016a). Sampling was carried out immediately after the coastal sampling (described below), covering one location per day during premonsoon and monsoon. Sampling for postmonsoon was carried out in a single day using a speed boat. Sampling during the premonsoon witnessed usual heavy but less frequent rainfall, whereas monsoon experienced copious amount of rainfall. Both premonsoon and monsoon sampling periods coincided with low-tide phase and therefore, considerable mixing of estuarine effluents with coastal Arabian Sea was expected. Unlike the two wet seasons, postmonsoon sampling featured dry period and coincided with high-tide phase.

2.1.2. Coastal Arabian Sea

Water samples for $\delta^{13}C_{DIC}$ and other parameters from the coastal Arabian Sea were collected during three cruises prior to the estuarine sampling onboard FORV–*Sagar Sampada* (SS-299, SS-306, and SS-311) covering premonsoon (12–20 April 2012), monsoon (1–12 September 2012) and postmonsoon (8–14 December 2012). These cruises were conducted to cover two transects viz. off Cochin and off Mangalore in the coastal Arabian Sea adjoining Cochin estuary and Netravati river, respectively (Fig. 1c). Six stations (station depths: 13, 20, 30, 40, 50, and 100 m) were occupied in both transects for sample collection from standard depths (surface, 10, 20, 30, 40, 50, 75, and 100 m; Fig. 1c and Table 1). The nearshore station in the Mangalore transect was closer to the coast (3.7 km) than off Cochin (10.4 km).

2.1.3. Data collection and sample analysis

The data for temperature and salinity during the study period were collected using a CTD profiler (model SBE 911 plus for the coastal and model SBE 25 for the Cochin estuary from Sea-Bird, USA). Water samples were collected using Niskin samplers connected to CTD Rosette for coastal locations. Samples for nutrients were pre-filtered using GF/F filters, which were analyzed spectrophotometrically for phosphate (P) and silicate (Si) (Thermo Evolution 201) within few hours of collection following standard procedures (Grasshoff et al., 1999). The analytical precision expressed as standard deviation, for P and Si were ± 0.02 and ± 0.03 μM, respectively. Samples for dissolved oxygen (DO) were collected in 60 ml glass bottles, fixed immediately with 0.5 ml each of Winkler reagents and titrated against 0.001 N thiosulphate with starch based visual end point detection (Grasshoff et al., 1999). The detection limit for DO was ± 2 μM.

During both estuary and coastal investigations, samples for pH, total alkalinity (TAlk), and $\delta^{13}C_{DIC}$ were collected in 125 ml reagent bottles. Samples were poisoned using saturated mercuric chloride (0.3 ml/60 ml) to arrest the microbial activity. Sample bottles were sealed using parafilm and kept in dark until analysis. The pH and TAlk (Dickson and Goyet, 1998) were measured using a Potentiometric Titrator (907 Titrando; Metrohm, Switzerland) calibrated on the NBS scale as described by Frankignoulle and Borges (2001). Analytical precision of pH for freshwater samples was ± 0.008 and for the rest ± 0.005. The measured values on NBS scale were first converted to in situ pH and then to the total scale. NIST certified reference standards were used for the calibration of pH while the certified reference material (Batch No. 111 supplied by Dr. A. G. Dickson of the Scripps Institution of Oceanography, USA) and internal standards (100–2000 $\mu mol\ kg^{-1}$ sodium carbonate) were used for the calibration of TAlk. The calibrations were performed for every tenth sample. Partial pressure of carbon dioxide (pCO_2) and DIC concentrations ([DIC]) were computed using the CO_2*SYS* program with the collected data on depth, temperature, salinity, P, Si, pH and TAlk using Millero et al. (2006) constants for whole salinity range.

2.1.4. $\delta^{13}C_{DIC}$ analysis

The measurements of $\delta^{13}C_{DIC}$ of the estuarine as well as coastal waters were performed using continuous flow isotope ratio mass spectrometer (Thermo Delta V plus) attached to a Gas-Bench system. Initially, 0.1 ml of 100% orthophosphoric acid taken in 12 ml glass vials was flushed with Helium at 28 °C. 1 ml of sample was transferred to the flushed vials carefully using a gas tight syringe by ensuring the absence

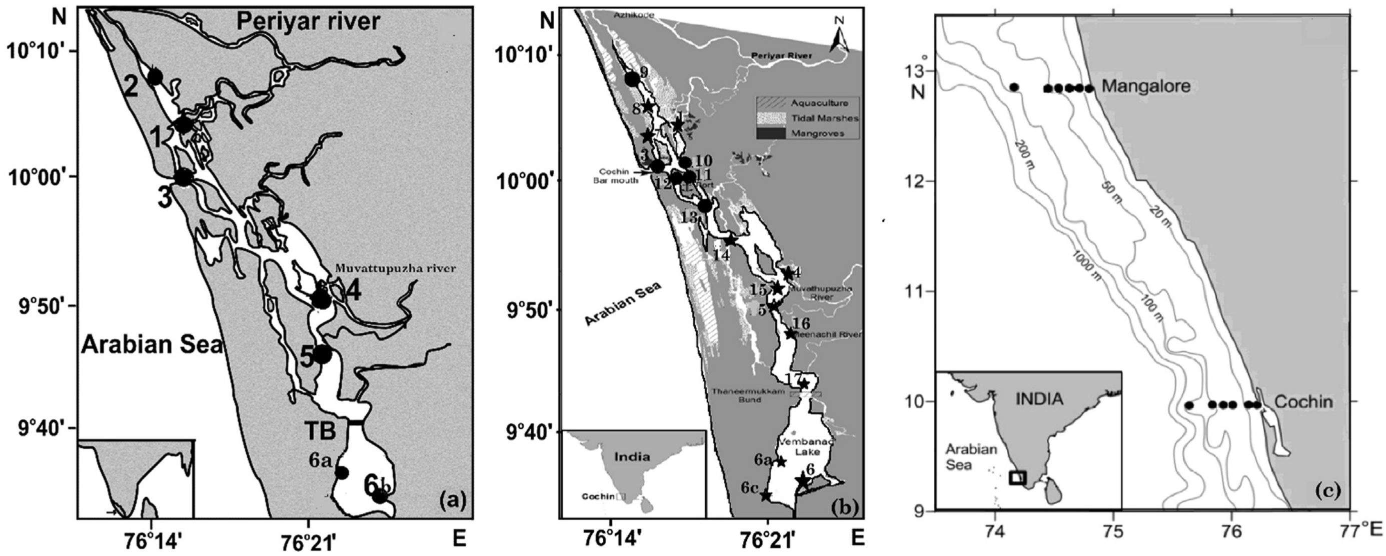

Fig. 1. Sampling locations in (a) Cochin estuary during premonsoon and monsoon, (b) Cochin estuary during postmonsoon (adapted from Bhavya et al., 2016a), and (c) sampling locations in the coastal Arabian Sea. Numbers in (a) indicate following stations: 1. Bolghatty-Periyar, 2. Null Zone, 3. Bar mouth, 4. Arikkutty, 5. Vaikom and 6 (a and b) Vembanad Lake. TB is Thannermukkam dam between Cochin estuary and Vembanad Lake. Circles in (b) indicate locations where calcite precipitation was dominant.

Table 1
Sampling locations in the coastal Arabian Sea.

Sample code	Station depth (m)	Geographical coordinates	Distance from the coast (km)	Sampling depth (m)	Geographical coordinates	Distance from the coast (km)	Sampling depth (m)
		Off Cochin			Off Mangalore		
1-0	13	09.969° N, 76.143° E	10.69	0	12.840° N, 74.793° E	3.89	0
1-10				10			10
2-0	20	09.967° N, 76.118° E	13.98	0	12.842° N, 74.739° E	9.65	0
2-10				10			10
2-20				20			20
3-0	30	09.967° N, 75.009° E	25.13	0	12.844° N, 74.678° E	16.32	0
3-10				10			10
3-20				20			20
3-30				30			30
4-0	40	09.970° N, 75.923° E	34.98	0	12.845° N, 74.616° E	23.08	0
4-10				10			10
4-20				20			20
4-30				30			30
4-40				40			40
5-0	50	09.970° N, 75.836° E	44.29	0	12.843° N, 74.493° E	36.59	0
5-10				10			10
5-20				20			20
5-30				30			30
5-40				40			40
5-50				50			50
6-0	100	09.964° N, 75.639° E	65.99	0	12.854° N, 74.160° E	72.39	0
6-10				10			10
6-20				20			20
6-30				30			30
6-40				40			40
6-50				50			50
6-60				N/A			60
6-75				75			75
6-100				100			100

of bubble. Subsequently, samples were kept in temperature bath for 18 h to ensure the complete extraction of CO_2 from the samples, which was then transferred to the mass spectrometer for isotopic analysis. The $\delta^{13}C$ was calculated based on the standard equation given below:

$$\delta^{13}C\ (‰) = \left(\frac{\mathrm{R_{Sample}} - R_{V-PDB}}{R_{V-PDB}}\right) \times 10^3$$

The analytical precision of $\delta^{13}C$ for replicate standards was better than 0.1‰. A well calibrated sodium carbonate salt ($\delta^{13}C$ = 11.4 ± 0.1‰) was used as laboratory standard.

Table 2
Different parameters in the Cochin estuary during sampling periods. The units of Si, P, and DO are in µM. TAlk and DIC are in µmol kg^{-1} and pCO_2 is in µatm. Temperature and $\delta^{13}C_{DIC}$ are in °C and ‰, respectively. Values at station 1 were considered as freshwater end members for the respective seasons during mixing model calculations.

Season	Stn.	Temp	pH	Salinity	DO	P	Si	DIC	TAlk	pCO_2	$\delta^{13}C_{DIC}$	SI (Ca)
Pre-monsoon	1	29.5	6.418	1.58	122.4	3.64	47.6	822	456	12,230	− 12.2	0.00
	2	29.9	7.255	15.6	150.0	2.95	42.1	1156	1104	2540	− 3.26	0.30
	3	30.1	7.325	13.0	127.2	2.68	41.1	916	882	1803	− 4.21	0.26
	4	30.6	6.920	6.27	213.2	0.51	48.5	584	496	3165	− 5.95	0.04
	5	29.1	6.402	5.31	201.0	0.30	70.9	357	218	4699	− 8.26	0.00
	6.a	29.4	6.030	0.26	194.9	0.54	113	1004	289	23,601	− 9.75	0.00
	6.b	29.4	6.523	0.53	212.0	0.57	90.2	777	308	7636	− 8.08	0.00
Monsoon	1	27.2	6.278	0.12	177.6	1.11	58.0	1191	477	22,316	− 13.6	0.00
	2	28.9	7.275	1.60	196.8	3.13	145	855	774	2832	− 8.27	0.05
	3	28.5	7.192	5.36	198.0	2.11	110	624	570	1955	− 5.69	0.07
	4	29.9	6.629	0.02	198.0	2.50	102	647	380	8932	− 9.28	0.00
	5	29.7	5.906	0.07	220.8	0.33	40.3	1301	284	33,796	− 9.25	0.00
	6.a	29.7	5.782	0.04	189.6	0.26	80.7	1633	278	45,015	− 11.7	0.00
	6.b	29.7	6.112	0.04	183.6	0.61	83.3	1216	372	28,067	− 11.8	0.00
Post-monsoon	1	27.9	7.050	0.12	274.7	2.30	107	697	438	1145	− 6.34	0.00
	3	27.8	8.058	32.3	232.7	0.47	10.4	1539	1729	439	0.79	3.14
	4	28.3	7.833	25.5	230.2	0.68	32.3	1029	1040	1094	− 1.12	0.59
	5	29.4	7.896	9.21	247.5	0.17	37.8	405	389	786	− 2.60	0.10
	6	29.8	6.994	1.92	242.6	0.43	76.3	403	238	5552	− 3.06	0.00
	6.a	30.3	6.414	0.91	200.5	0.38	73.3	343	259	7229	− 4.93	0.00
	6.c	29.6	6.413	1.89	240.1	0.33	79.6	473	265	6966	− 3.81	0.00
	7	27.7	7.570	23.0	277.2	0.69	25.5	1233	1304	1946	− 3.12	0.97
	8	27.9	7.619	24.5	230.2	1.20	55.3	1355	1379	1170	− 2.17	0.93
	9	28.0	7.964	29.8	264.8	0.39	56.2	1461	1597	536	0.22	2.36
	10	30.1	7.547	9.37	316.8	0.82	16.4	1297	1345	570	− 3.69	1.53
	11	29.3	8.017	24.2	309.4	0.70	18.4	1243	1334	545	− 0.23	1.73
	12	29.3	7.914	25.4	240.1	0.53	21.6	1584	1711	602	− 0.38	2.52
	13	27.8	7.968	32.1	220.3	0.69	29.3	1275	1371	629	0.48	1.59
	14	28.0	7.527	20.2	195.5	0.27	36.0	522	499	1198	− 1.92	0.12
	15	29.3	7.202	10.5	324.2	0.27	40.1	546	502	1704	− 5.35	0.08
	16	29.0	7.130	11.1	193.1	0.35	45.5	439	461	242	− 4.13	0.41
	17	29.3	7.364	9.77	302.0	0.16	37.1	422	374	1767	− 2.73	0.04

3. Results

3.1. Cochin estuary

Surface water temperature in the Cochin estuary varied in a narrow range during the present study with the lowest around 27.2 °C in the monsoon (Stations 1) to the highest around 30.6 °C during premonsoon (Station 4; Table 2). Due to usual premonsoon rains the estuary resembled early monsoon conditions with low salinity in the upper estuary and at the river meeting stations. Relatively high saline conditions during premonsoon were mostly restricted near both sea inlet stations (Fig. 1; Table 2). The estuary turned into a freshwater system during monsoon with the highest salinity of 5.36 near the bar mouth (station 3). The postmonsoon witnessed the highest salinity of 32.3 near the bar mouth and declined to 0.12 at Station 1 (Table 2). Vembanad Lake showed consistently low salinity with seasonal average values ranging between 0.04 and 1.57 throughout the study period (Table 2). Silicate concentration in the estuary was the highest during monsoon (average ~ 91 ± 42 µM) followed by premonsoon (50 ± 12 µM) and postmonsoon (37 ± 23 µM). The Si concentrations in the Vembanad were > 73 µM throughout the year. The P concentrations in the estuary were high during premonsoon (average ~ 2.0 ± 1.51 µM) and monsoon (1.85 ± 1.12 µM) with higher values in the north compared to the south (Table 2). Postmonsoon had the lowest P (0.65 ± 0.53 µM). Vembanad Lake showed low P throughout (< 0.6 µM).

The estuarine pH was higher during postmonsoon (7.050–8.058) compared to premonsoon (6.402–7.325) and monsoon (5.906–7.275; Table 2). In general, pH was higher in the northern part of the estuary (Stations 1–3) compared to the southern (Stations 4–5). Freshwater Vembanad Lake consistently showed acidic pH (premonsoon: 6.030–6.523; monsoon: 5.782–6.112; postmonsoon: 6.413–6.994). TAlk was higher during postmonsoon (average ~ 1032 ± 525 µmol kg^{-1}) followed by premonsoon (631 ± 356 µmol kg^{-1}) and monsoon (497 ± 188 µmol kg^{-1}). In general, the northern estuary showed higher TAlk compared to the southern estuary and Vembanad Lake (Table 2). DO in the estuary was relatively higher during postmonsoon (257 ± 42 µM) compared to premonsoon (163 ± 42 µM) and monsoon (198 ± 15 µM). DO in the Vembanad was in the same range as the rest of the estuary.

The [DIC] in the estuary were lower during the premonsoon (average ~ 767 ± 307 µmol kg^{-1}) compared to the monsoon (923 ± 310 µmol kg^{-1}) and the postmonsoon (1003 ± 445 µmol kg^{-1}) with higher values generally towards the north compared to the south. Vembanad Lake showed lower [DIC] during postmonsoon (< 473 µmol kg^{-1}) and increased by more than three times during monsoon (> 1216 µmol kg^{-1}). pCO_2 in the estuary ranged from 1803 to 12,230 µatm, 1955 to 33,796 µatm, and 439–1946 µatm during the premonsoon, monsoon and postmonsoon, respectively. pCO_2 observed in the southern estuary (33,796 µatm) and the Vembanad Lake (28,067–45,051 µatm) during monsoon are among the highest values reported in the Indian estuaries. $\delta^{13}C_{DIC}$ in the estuarine region ranged from − 12.2 to − 3.26‰ during the premonsoon with an average of − 6.78 ± 3.59‰. A comparable range (− 13.6 to − 5.69‰) was observed during the monsoon with slightly lower average of − 9.23 ± − 2.87‰. Comparatively higher $\delta^{13}C_{DIC}$ (− 2.15 ± 2.14‰) was observed during the postmonsoon with the highest $\delta^{13}C_{DIC}$ observed for the Cochin estuary (0.79‰) at the bar mouth (station 3; Fig. 2; Table 2).

3.2. Coastal Arabian Sea

The data for different parameters in surface waters of the coastal transects are given in Tables 3, 4. The sea surface temperature in the coastal transects was the lowest during monsoon (Cochin: 25.8–27.4 °C; Mangalore: 26.8–27.5 °C) followed by postmonsoon (Cochin:

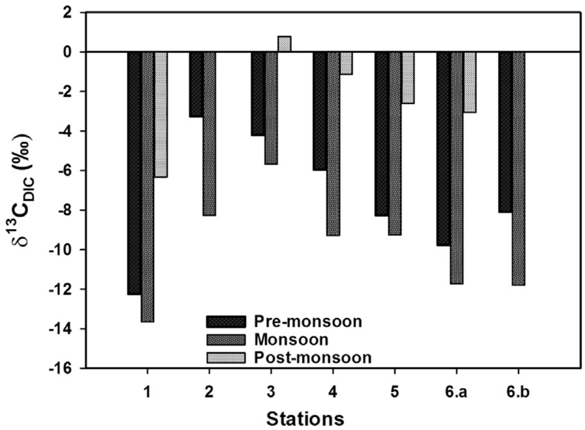

Fig. 2. Variations in $\delta^{13}C_{DIC}$ of the Cochin estuary during three seasons. Postmonsoon values at locations other than shown above is tabulated in Table 2.

29.5–30.2 °C; Mangalore: 29.3–29.8 °C) and premonsoon (Cochin: 30.1–30.7 °C; Mangalore: 30.1–31.4 °C). The salinity patterns of the coastal Arabian Sea clearly show impacts of monsoon driven freshwater inflow on the coastal waters. Surface salinity during monsoon was lower (Cochin: 31.7–34.1; Mangalore: 27.1–33.1) compared to premonsoon (Cochin: 33.9–35.0; Mangalore: 34.6–35.2) and postmonsoon (Cochin: 33.8–35.0; Mangalore: 34.6–35.2). The lowest salinity was at nearshore locations during monsoon. Average surface water pH in the off Cochin transect during premonsoon (8.132 ± 0.015) and monsoon (8.101 ± 0.160) was less than that of the off Mangalore transect (premonsoon: 8.139 ± 0.013 and monsoon: 8.144 ± 0.022), whereas the opposite was observed during the postmonsoon (off Cochin: 8.165 ± 0.008 and off Mangalore: 8.124 ± 0.068).

Si concentrations in the surface water of the Cochin transect was high during postmonsoon (5.86 ± 3.38 µM) and monsoon (4.0 ± 2.61 µM) and decreased significantly during premonsoon (0.96 ± 0.39 µM). The Si was the highest at nearshore location during postmonsoon in the Cochin transect (Table 3). On the contrary, surface Si concentration in the Mangalore transect was the highest during premonsoon (3.35 ± 1.34 µM) followed by monsoon (2.67 ± 2.12 µM) and postmonsoon (1.96 ± 0.69 µM). Unlike Si, P in Cochin transect, was the lowest during postmonsoon (0.10 ± 0.03 µM) to increase in the monsoon (0.42 ± 0.30 µM) and premonsoon (0.31 ± 0.16 µM). P in the Mangalore transect was almost similar during all three seasons (premonsoon: 0.28 ± 0.22 µM; monsoon 0.20 ± 0.16 µM; postmonsoon 0.23 ± 0.19 µM). DO in surface waters was higher than 130 µM throughout the year (136–285 µM) in both Cochin and Mangalore transects, except at surface waters of 40 m water depth station where it was anomalously low (41.5 µM).

In general, depth-wise pCO_2 during the premonsoon (off Cochin: 417–720 µatm; off Mangalore: 404–844 µatm) and the monsoon (off Cochin: 254–1052 µatm; off Mangalore: 393–1220 µatm) were in higher range than the postmonsoon (off Cochin: 395–598 µatm; off Mangalore: 401–855 µatm). Contrary to estuarine waters, surface [DIC] in the coastal waters varied in a narrow range (1749–2115 µmol kg^{-1}) on annual scale (Tables 3, 4). Surface $\delta^{13}C_{DIC}$ during premonsoon was comparable in both off Cochin (0.72–1.07‰) and off Mangalore (0.81–1.13‰). In contrast, during the monsoon, surface $\delta^{13}C_{DIC}$ off Cochin witnessed a wider range (− 0.20–2.02‰) compared to off Mangalore (0.76–1.19‰). During postmonsoon, the scenario was different with relatively higher $\delta^{13}C_{DIC}$ at off Cochin (0.27–1.15‰) compared to off Mangalore (0.04–1.08‰; Tables 3, 4). The depth profiles of $\delta^{13}C_{DIC}$ in the coastal Arabian Sea are shown in Fig. 3.

4. Discussion

The prevailing eutrophication and augmented heterotrophy in the Cochin estuary persuaded researchers to focus on the C dynamics of this ecosystem (Gupta et al., 2009). The results from studies so far revealed that the Cochin estuary is a vulnerable ecosystem with amplified primary productivity, decreased oxygen level, increased bacterial activities, OM degradation, species shift, and supersaturation of CO_2 (Thottathil et al., 2008; Gupta et al., 2009; Martin et al., 2013; Bhavya et al., 2016a, 2016b, 2017). However, many detailed aspects of C cycling of this eutrophic ecosystem remains understudied such as major processes affecting $\delta^{13}C_{DIC}$ and [DIC] in the estuary. For this purpose, we employed the concept of mixing curve approximation (Alling et al., 2012) in the estuary through our data and findings are discussed below.

Under conservative mixing, the values of DIC and $\delta^{13}C_{DIC}$ at a particular location are assumed to be independent of the local biogeochemical processes, but are dependent on the fraction of each end members (sources) at that place. In an estuary, likely dominant sources controlling DIC dynamics are the waters of two different salinities; i.e., freshwater and seawater. Accordingly, during the present study, $\delta^{13}C_{DIC}$ and [DIC] values at the meeting point of the Periyar river (the major river draining into the estuary) with the estuary have been considered as freshwater end member. Average of surface $\delta^{13}C_{DIC}$ and [DIC] at 30, 40, 50 and 100 m depth stations of the coastal transect have been

Table 3
Different parameters in the surface waters of the off Cochin transect during the three sampling periods. The units of P, Si, and DO are in µM. DIC is in µmol kg^{-1} and pCO_2 in µatm. Temperature and $\delta^{13}C_{DIC}$ are in °C and ‰, respectively. The average of surface values at locations C3-0, C4-0, C5-0 and C6-0 for the respective seasons (except C4-0 during monsoon) were considered as seawater end members during mixing model calculations.

Season	Stn	Temp (°C)	pH	Salinity	DO	P	Si	DIC	pCO_2	$\delta^{13}C_{DIC}$
Pre monsoon 2012	C1-0	30.2	8.103	33.9	179.3	0.52	1.59	2008	514	0.93
	C2-0	30.1	8.133	34.0	187.7	0.33	1.26	1874	444	0.72
	C3-0	30.4	8.130	34.5	186.7	0.50	0.68	1927	459	0.86
	C4-0	30.7	8.133	34.8	183.0	0.21	0.49	1944	459	0.90
	C5-0	30.2	8.140	34.8	220.4	0.22	0.85	1982	458	1.00
	C6-0	30.1	8.150	35.0	211.0	0.11	0.94	1958	442	1.07
Monsoon 2012	C1-0	25.8	7.981	31.7	136.6	0.43	8.03	2024	690	0.03
	C2-0	26.2	8.176	31.7	232.0	0.28	3.86	1786	377	0.89
	C3-0	26.3	8.322	31.9	285.5	0.19	3.19	1749	254	2.02
	C4-0	25.9	7.865	34.1	41.37	1.02	6.01	2115	936	− 0.20
	C5-0	26.7	8.126	33.1	214.2	0.36	1.45	1953	464	0.98
	C6-0	27.4	8.139	33.7	197.1	0.27	1.41	2003	459	1.10
Post monsoon 2012	C1-0	29.9	8.156	35.0	196.8	0.17	10.8	1916	436	0.32
	C2-0	29.6	8.178	34.6	147.2	0.08	8.71	1862	395	0.95
	C3-0	29.5	8.168	33.8	222.1	0.09	6.39	1882	407	0.99
	C4-0	29.5	8.165	34.0	221.5	0.07	4.18	1945	423	0.72
	C5-0	30.2	8.156	33.9	201.6	0.11	2.04	1921	429	1.15
	C6-0	29.7	8.165	34.7	198.9	0.13	3.13	1924	417	0.27

Table 4
Different parameters in the surface waters of the off Mangalore transect during the three sampling periods. The units of P, Si, and DO are in μM. DIC is in μmol kg^{-1} and pCO_2 in μatm. Temperature and $\delta^{13}C_{DIC}$ are in °C and ‰, respectively.

Season	Stn	Temp (°C)	pH	Salinity	DO	P	Si	DIC	pCO_2	$\delta^{13}C_{DIC}$
Pre monsoon 2012	M1-0	31.4	8.125	35.2	187.7	0.40	5.29	1832	442	1.00
	M2-0	31.0	8.121	35.0	180.9	0.44	3.76	1827	446	0.81
	M3-0	31.0	8.145	34.9	182.6	0.21	3.46	1960	450	0.96
	M4-0	30.5	8.144	34.7	185.1	0.57	3.96	1816	417	1.01
	M5-0	30.1	8.150	34.6	209.5	0.05	1.94	1917	433	1.03
	M6-0	30.1	8.151	35.0	206.5	0.03	1.70	1924	431	1.13
Monsoon 2012	M1-0	26.9	8.146	27.1	167.2	0.40	3.03	1697	404	0.76
	M2-0	27.5	8.109	29.8	174.5	0.40	6.68	1804	462	0.95
	M3-0	27.0	8.143	30.7	182.6	0.21	2.55	1840	428	0.91
	M4-0	27.2	8.159	31.5	195.4	0.12	1.30	1803	400	0.89
	M5-0	26.8	8.136	32.2	189.4	0.05	1.68	2018	471	1.19
	M6-0	27.2	8.175	33.1	192.2	0.03	0.82	1867	393	1.02
Post monsoon 2012	M1-0	29.3	8.001	34.6	150.8	0.63	2.58	1920	626	0.04
	M2-0	29.3	8.087	34.9	173.9	0.28	1.78	1919	504	0.88
	M3-0	29.3	8.148	35.0	188.4	0.18	1.06	1880	424	0.55
	M4-0	29.8	8.170	35.1	205.7	0.13	2.32	1880	401	0.48
	M5-0	29.3	8.169	35.0	205.3	0.11	2.75	1912	408	1.08
	M6-0	29.4	8.171	35.2	201.2	0.11	1.30	1931	409	0.54

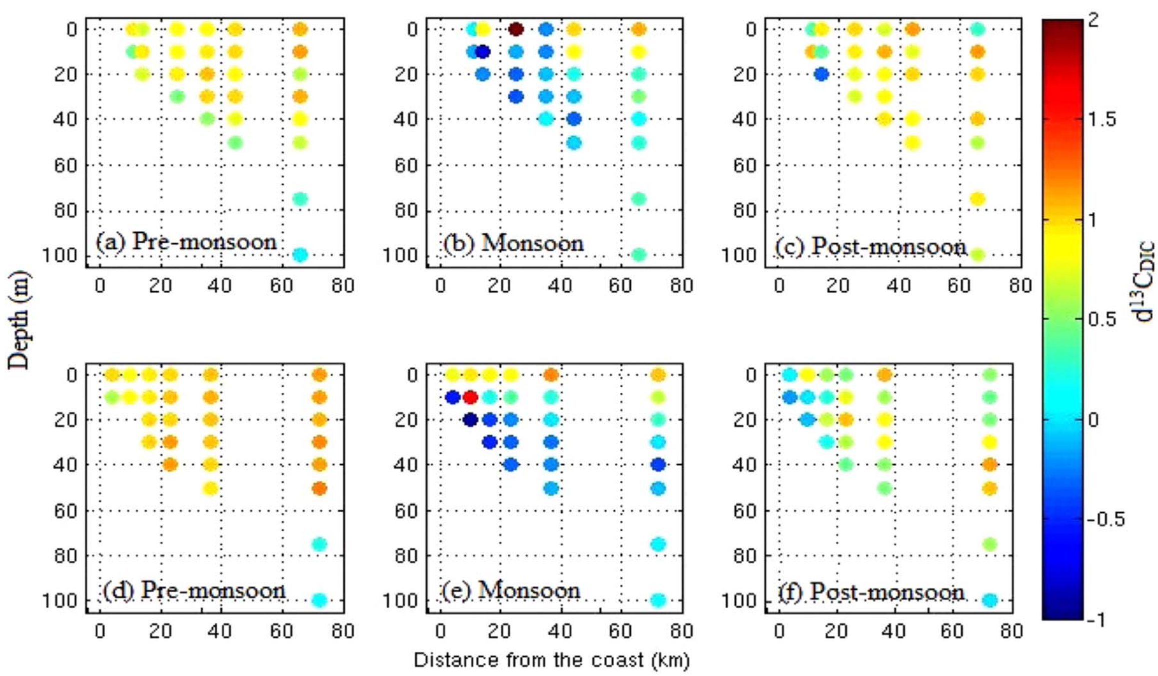

Fig. 3. Depth profiles of $\delta^{13}C_{DIC}$ in the coastal Arabian Sea; a–c are the depth profiles in the Cochin transect during premonsoon, monsoon, and postmonsoon, respectively; d–f are the same for Mangalore transect.

considered as seawater end member for $\delta^{13}C_{DIC}$ and [DIC] during respective seasons. The Vembanad Lake, despite being freshwater system, was not considered as freshwater end member as this was an isolated freshwater body separated by a dam and lacked active interaction with the saline regions of the estuary. To create a hypothetical mixing curve for [DIC] and $\delta^{13}C_{DIC}$, we assumed that the salinity at particular location is dominantly dependent on the fraction of freshwater mixed with seawater (F_{fw}). To calculate the mixing curve and signatures of biogeochemical processes as discussed below, we followed Alling et al. (2012). F_{fw} can be calculated using the mass balance equation for salinity (Eq. (1)).

$$S_{mix} = S_{fw}F_{fw} + S_{sw}(1-F_{fw}) \quad (1)$$

Where, S_{mix} is the salinity measured at each station, S_{fw} and S_{sw} represent the salinities of freshwater and seawater end members, respectively. Using F_{fw}, we calculated the conservative mixing values of [DIC] and $\delta^{13}C_{DIC}$ (Eqs. (2) and (3), respectively).

$$[DIC]_{mix} = [DIC]_{fw}F_{fw} + [DIC]_{sw}(1\text{-}F_{fw}) \quad (2)$$

$$\delta^{13}C_{mix} = \frac{[DIC]_{fw}\delta^{13}C_{fw}F_{fw} + [DIC]_{sw}\delta^{13}C_{sw}(1-F_{fw})}{[DIC]_{fw}F_{fw} + [DIC]_{sw}(1-F_{fw})} \quad (3)$$

Where [DIC] is the concentration of DIC, subscripts 'sw' and 'fw' denotes the seawater and freshwater, respectively. The subscript 'mix' represents the conservative mixing value at any point between the end members in the estuary. The $\delta^{13}C_{mix}$ is a theoretical value of $\delta^{13}C_{DIC}$, where there are no sources or sinks of DIC and is purely a function of salinity and [DIC] of the two end members (Eq. (3)). Fig. 4a and b show the variation of measured and conservative mixing values of [DIC] and $\delta^{13}C_{DIC}$, respectively, with salinity in the estuary for all three seasons.

Fundamentally, DIC fraction would decrease if primary productivity exceeds respiration due to consumption of DIC during C fixation, whereas $\delta^{13}C_{DIC}$ is expected to increase under this condition due to excess removal of lighter isotope (^{12}C). From preliminary analysis, it

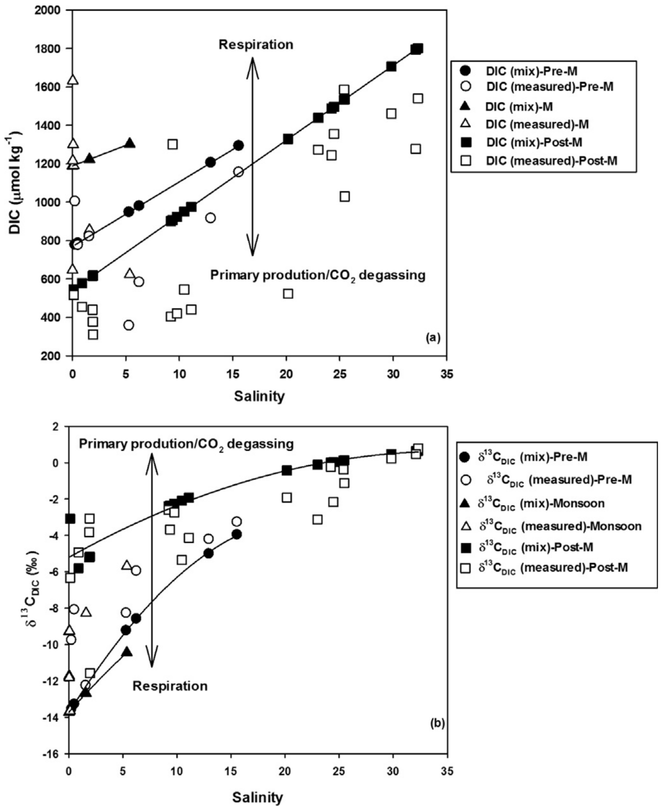

Fig. 4. (a) DIC concentrations in the Cochin estuary against salinity, and (b) $\delta^{13}C_{DIC}$ against salinity. Filled and open symbols indicate conservative mixing and measured values, respectively. The arrows indicate the influence of primary productivity and OM degradation on the isotopic composition and concentrations of DIC. Pre-M and Post-M indicate premonsoon and postmonsoon, respectively.

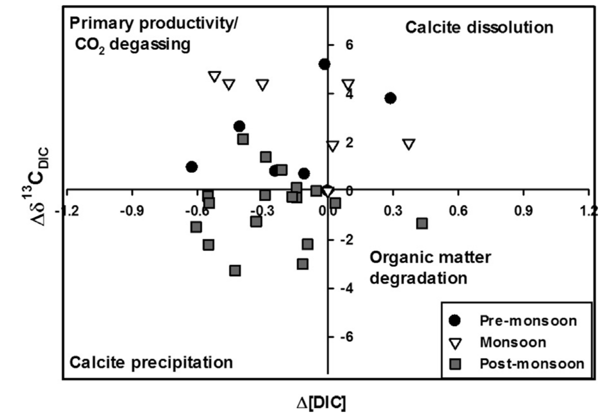

Fig. 5. Deviations in $\delta^{13}C_{DIC}$ ($\Delta\delta^{13}C_{DIC}$) versus DIC concentrations (Δ[DIC]) from the corresponding conservative mixing values in the Cochin estuary. The four quadrants depict the processes which are most likely to affect the $\delta^{13}C_{DIC}$ in the estuary.

appears that the [DIC] and $\delta^{13}C_{DIC}$ are predominantly controlled by primary productivity and OM degradation (Fig. 4a and b). However, there are several other estuarine processes occurring simultaneously that may also play a major role in modulating the C dynamics of the system. Hence, it is prudent to understand these processes using advanced modeling approach. Erlenkeuser et al. (2003) have reported that the deviation of [DIC] and $\delta^{13}C_{DIC}$ from the conservative mixing value can be used as a proxy to understand the processes in a detailed manner. Eqs. (4) and (5) below has been used to calculate these deviations, i.e., $\Delta\delta^{13}C_{DIC}$ and Δ[DIC].

$$\Delta\delta^{13}C_{DIC} = \delta^{13}C_{sample} - \delta^{13}C_{mix} \tag{4}$$

$$\Delta[DIC] = \frac{[DIC]_{sample} - [DIC]_{mix}}{[DIC]_{mix}} \tag{5}$$

Fig. 5 shows the $\Delta\delta^{13}C_{DIC}$ of the samples plotted against the corresponding Δ[DIC] values. The data points are spread in four quadrants with reference to the major processes controlling them. In general, locations where $[DIC]_{sample} > [DIC]_{mix}$, indicate the addition of DIC to the existing pool, whereas the opposite is true for sinks.

Samples which fall in the upper left quadrant indicate the $^{13}C_{DIC}$ enrichment along with decrease in the [DIC] concentration, which could be due to degassing of CO_2 and primary production. During the present study, it appears that the estuarine $\delta^{13}C_{DIC}$ and [DIC] during the wet seasons (premonsoon and monsoon) were mainly controlled by degassing of CO_2 and freshwater mixing. Cochin estuary turns into a freshwater system during wet seasons, with low $\delta^{13}C_{DIC}$ (Fig. 4b) negatively correlated with [DIC] (R^2 = 0.48 for monsoon; Fig. 6a). It shows that DIC brought in by freshwater leads to dilution of ^{13}C in the estuarine DIC pool (Fig. 4b). This is also corroborated by negative trend between $\delta^{13}C_{DIC}$ and Si (R^2 = 0.31; Fig. 6b), where locations with increased Si concentrations, evidence of freshwater input, showed lower $\delta^{13}C_{DIC}$. However, $\delta^{13}C_{DIC}$ and P did not show any trend (Fig. 6c), probably because of dynamic biogeochemistry of P in the estuary (Bhavya et al., 2016b).

Positive relationship between $\delta^{13}C_{DIC}$ and DO during monsoon (R^2 = 0.35; Fig. 6d) suggest role of respiration in regulating the DIC dynamics in the estuary, especially during the wet seasons. Respiration led to consumption of DO and addition of ^{13}C depleted DIC to the estuarine DIC pool resulting into lower $\delta^{13}C_{DIC}$. Respiration is known to dominate primary productivity in the Cochin estuary (primary production: respiration < 1) during wet seasons, particularly during monsoon, leading to heterotrophic conditions (Thottathil et al., 2008). Despite this, limited number of data points in the lower right quadrant does not mean the absence of OM degradation. Studies show that Indian estuaries mineralize up to 90% of terrestrial organic loads during high-flow conditions (Gupta et al., 2008). This results in higher pCO_2 during the high flow periods with plenty of lateral inputs bringing excess OM. The excess CO_2 thus brought from freshwater and produced in situ through respiration is effluxed out. Station 1 situated at the outlet point of the Periyar River and reception point of surplus anthropogenic OM exhibited high pCO_2 during wet season. Although smaller in comparison, the Muvattupuzha River also appears to have brought enough OM to Station 4. Moreover, the mesohaline zones (salinity 10–20) of this eutrophic estuary receive several fold higher anthropogenic (lateral) inputs of OM compared to riverine inputs (Thottathil et al., 2008; Gupta et al., 2009). But only five data points out of entire current study represented this mesohaline region which probably are insufficient for the mixing model to properly exhibit OM degradation. Therefore, the mixing model infers that the C-dynamics in this estuary during wet seasons are heavily influenced by the acidic fresh water runoff followed by in situ metabolism.

$RpCO_2$, the ratio of pCO_2 in the aqueous medium to atmospheric pCO_2 (~ 390 µatm) can provide a clue about an ecosystem being a source or sink of CO_2 (Samanta et al., 2015). In general, during premonsoon and monsoon, most of the stations are CO_2 supersaturated showing very high $RpCO_2$ with lower salinity indicating potential CO_2 degassing from the system (Fig. 7). Most of the postmonsoon stations, however, show relatively higher salinity and [DIC] along with low $RpCO_2$ indicating the intrusion of seawater and possible dominance of primary productivity over OM degradation. Relatively enriched $\delta^{13}C_{DIC}$ at such locations are also in agreement with this hypothesis.

The lower left quadrant represents the calcite precipitation, where both [DIC] and $\delta^{13}C_{DIC}$ decreased (Fig. 5; Alling et al., 2012). However, locations undergoing high OM degradation with simultaneous CO_2 degassing can also fall into this quadrant. To ascertain the locations undergoing calcite precipitation during the present study, Calcite

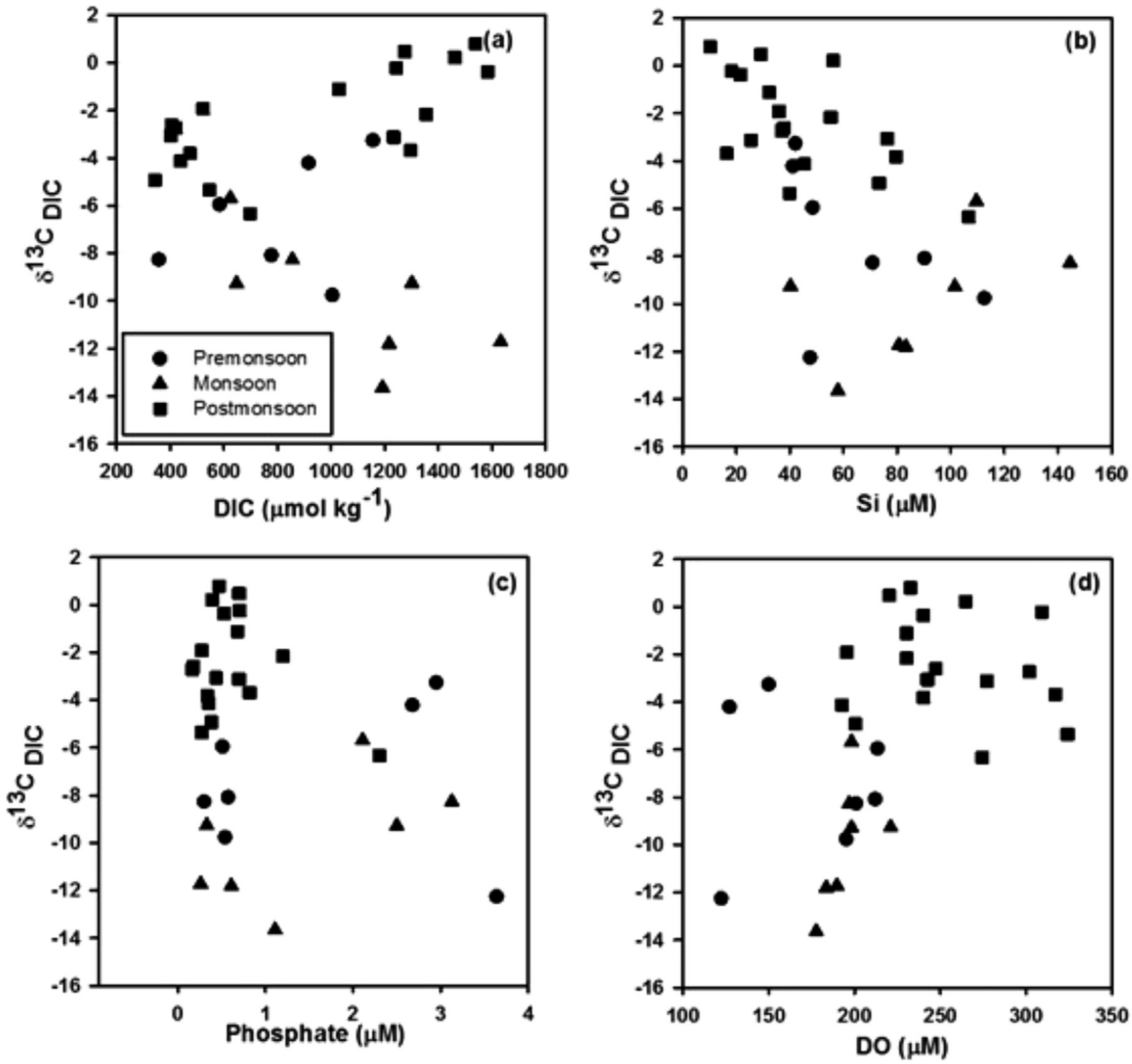

Fig. 6. Relationship between (a) $\delta^{13}C_{DIC}$–DIC (R^2 = 0.48 for monsoon), (b) $\delta^{13}C_{DIC}$–Si (R^2 = 0.31), (c) $\delta^{13}C_{DIC}$–Phosphate, and (d) $\delta^{13}C_{DIC}$–DO (R^2 = 0.35 for monsoon) in the Cochin estuary during the study period.

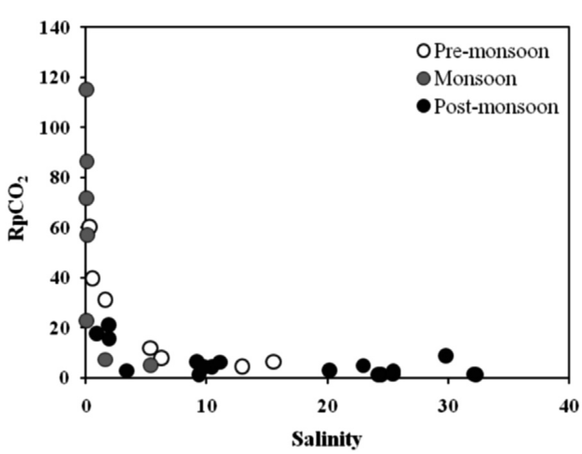

Fig. 7. $RpCO_2$ variations with salinity in the estuary during the study period.

Saturation Index (SI_{Ca}) was calculated using CO_{2SYS} program (Lewis et al., 1998), where calcium concentration is assumed to be directly proportional to salinity. $SI_{Ca} > 1$ indicates calcite oversaturation whereas $SI_{Ca} < 1$ indicates undersaturation. SI_{Ca} in the estuary varied between 0 and 0.30 (premonsoon), 0–0.07 (monsoon), and 0–3.14 (postmonsoon). Six postmonsoon locations of upper estuary falling in the lower left quadrant (Fig. 5) show $SI_{Ca} > 1$ confirming the contribution of calcite precipitation in modulating the $\delta^{13}C_{DIC}$ in this zone abundant with bottom bivalve shells (Gupta et al., 2009). Rest of the sampling stations show calcite undersaturation throughout the year. The highest $\delta^{13}C_{DIC}$ observed at the bar mouth (station 3) during postmonsoon appears to carry marine signature due to high tide condition during sampling and reduction in freshwater supply.

The upper right quadrant represents the stations with calcite dissolution as the major process. $\Delta\delta^{13}C_{DIC}$ and Δ[DIC] > 0 at these stations indicate increase in [DIC] as well as enrichment of ^{13}C. These are stations with relatively low pH and higher pCO_2 levels (stations 5, 6a and 6b). Incidentally, the macro benthos of this region is heavily dominated with bivalves (~ 50%, Martin et al., 2010), so calcite dissolution is regarded as an important CO_2 source here at low pH conditions. Dissolution of carbonate minerals was also reported in other estuaries such as the Godavari estuary (Bouillon et al., 2003), the Loire (Abril et al., 2003) and the Ems estuary (de Jonge and Villerius, 1989). However, Abril et al. (2003) observed carbonate dissolution in the low saline region, whereas Bouillon et al. (2003) and de Jonge and Vilerius (1989) observed this effect in the low to middle salinity zone.

The pCO_2 values during the present study 23,601–45,015 μatm) in the Vembanad Lake during premonsoon and monsoon are higher than

pCO_2 21,997–34,026 μatm) measured in the upstream of the Godavari estuary (Sarma et al., 2011) during wet seasons. The major process regulating distribution of CO_2 in the central Vembanad Lake (Cochin Estuary) is net ecosystem metabolism (Gupta et al., 2009). It has been shown that increased bacterial respiration due to lateral inputs caused by anthropogenic activities has led to CO_2 super-saturation in the mesohaline regions of this estuary (Thottathil et al., 2008), though its corresponding estimates from the southern Vembanad Lake are not available. Further, the sediments in the southern Vembanad Lake and its adjacent paddy fields (Kuttanad) have become acidic due to inadequate flushing of alkaline sea water by Thanneermukkam dam (Fig. 1a). Therefore, it is possible that the acidic effluents from the aquaculture fields and seepage from inter-tidal sediments during peak discharge season could lower the pH and increase the pCO_2 levels.

Taken together, the major processes controlling DIC dynamics in the Cochin estuary are OM degradation and CO_2 degassing during premonsoon and monsoon. Calcium carbonate precipitation is a dominant process during postmonsoon. However, these findings can be influenced by the selection of freshwater inputs. Since the Cochin estuary receives OM loading from other small rivers and tributaries, the C dynamics in this estuary can be significantly influenced by them as well. During our analysis we have assumed the Periyar river as the freshwater end member. Therefore, these results can be taken as a preliminary identification of major processes responsible for variability in [DIC] and its isotopic composition in this tropical estuary.

4.1. Coastal Arabian Sea and estuarine-coastal coupling

The biogeochemistry of the coastal Arabian Sea, especially the nearshore environment, is significantly influenced by the discharges from the Cochin estuary (Bhavya et al., 2016b, 2017). It has been reported earlier that coastal ecosystem of the west coast of India is significantly perturbed with anthropogenic inputs chiefly contributed by the fertilizer runoff (Naqvi et al., 2009). However, our parallel studies from the Cochin estuary showed that it is a zone of heavy sink for anthropogenic nutrients as evidenced by very fast turnover rates of nitrogen (Bhavya et al., 2016b), thereby restricting its influence to the nearshore regions. Studies from other Indian monsoonal estuaries also showed that they efficiently retain about 90% of anthropogenic nutrients thereby their export fluxes are very low especially to the Arabian Sea compared to the Bay of Bengal (Krishna et al., 2016). A clear presence of surface depleted DO and $\delta^{13}C_{DIC}$ associated with high pCO_2 at station 1 (nearshore, ~ 10 km away from the coast) and drastic dilution of such signals to station 2 (~ 3.3 km away from station 1) during monsoon (Table 3) shows that Cochin estuarine influence is not significantly extended beyond nearshore region even under high runoff conditions. Although low surface saline condition was seen extended up to station 3 (25 km away from the coast, Table 3), the runoff associated inputs are quickly removed before crossing the nearshore region. This is supported by high C and N uptake rates in the nearshore regions of both Cochin and Mangalore (Bhavya et al., 2016b, 2017) and lower rates at the farther stations.

Seasonal distribution of $\delta^{13}C_{DIC}$ over the Cochin and Mangalore shelves showed relatively lower values in the subsurface waters even at the farthest stations during monsoon, but it only sparsely depleted off Mangalore during postmonsoon (Fig. 3). When terrestrial influence is confined mostly to the nearshore regions, the lower subsurface $\delta^{13}C_{DIC}$ throughout the shelf indicates that they are impacted by offshore processes. Coastal regions along west coast of India experiences upwelling during monsoon (June–September), which brings cool and highly mineralized offshore oxygen minimum zone (OMZ) waters onto the shelf (Gupta et al., 2016; Sudheesh et al., 2016). Being mineralized, these OMZ waters depleted with oxygen and relatively lower $\delta^{13}C_{DIC}$ advect over these shelf regions under the advent of upwelling. The upwelled nutrients enhance phytoplankton production and their eventual mineralization (Gupta et al., 2016) further depletes subsurface $\delta^{13}C_{DIC}$ (Fig. 3). Despite being highly productive these coastal regions are a source of CO_2 to the atmosphere during monsoon (Table 3) as the supply of CO_2 from the upwelling is higher than its drawdown by phytoplankton.

Interestingly, station 4 off Cochin during monsoon displayed unusually low $\delta^{13}C_{DIC}$ and DO associated with high DIC and pCO_2 whereas its adjoining station 3 displayed vice versa conditions (Table 3; Fig. 3). This monsoon sampling period encountered with an episodic event wherein most parts of beaches along this coast were exposed for two days due to unusual retrieval of seawater (less saline) which was felt up to station 3. Usually the upwelled waters (cool, high saline, depleted with DO and $\delta^{13}C_{DIC}$) from offshore advect along the bottom and reach to surface near coast, but in this instance the opposite force (sea retrieval) from the coast prevented upwelling, advection instead got uplifted to surface at station 4 (see Fig. 14, Gupta et al., 2016). This resulted in a temporary steep thermohaline gradient between these stations that restricted the phytoplankton production at station 4 (Chlorophyll: 0.97 mg m^{-3}) but steeply enhanced at station 3 (Chlorophyll: 8.2 mg m^{-3}; Gupta et al., 2016). This high localized primary productivity led to surface enrichment of ^{13}C in DIC and undersaturation of CO_2 at station 3.

Relative to Cochin the Mangalore subsurface and outer shelf waters are more depleted in ^{13}C with lower $\delta^{13}C_{DIC}$ (Fig. 3) as this shelf experiences intrusion of relatively highly mineralized and oxygen depleted upwelled waters compared to the Cochin (Gupta et al., 2016; Sudheesh et al., 2016). Further oxygen demand (for respiration of sinking plankton) on already depleted upwelled waters turns these subsurface shelf waters to anoxic up to about 60 km from the coast. The highest ^{13}C depletion in DIC at the near shore bottom waters of Mangalore during the monsoon (Fig. 3e) may be due to the strong sulfate reduction in these highly anoxic waters/sediments (Naqvi et al., 2009).

The average surface $\delta^{13}C_{DIC}$ values of coastal waters during premonsoon, monsoon, and postmonsoon (Cochin: 0.91 ± 0.11, 0.80 ± 0.80 and 0.73 ± 0.42‰; Mangalore: 0.99 ± 0.10, 0.95 ± 14, and 0.60 ± 0.35‰, respectively; Tables 3, 4) are lower than the model predicted open ocean values (1.64‰; Sonnerup et al., 2000). Previous studies have reported that the Arabian Sea is a source of CO_2 to the atmosphere (Sarma, 2003; Takahashi et al., 2009; Valsala and Maksyutov, 2010; Sarma et al., 2012) hence, the oceanic Suess effect can be neglected. Therefore, $\delta^{13}C_{DIC}$ in the coastal Arabian Sea is most likely dependent on physical and biological processes rather than atmospheric CO_2 concentration. To confirm this hypothesis, we used a similar (as for Cochin estuary) mixing curve approximation for the Cochin coastal transect. Like in the estuary, the Periyar River and average surface seawater values have been taken as freshwater and seawater end members, respectively. Fig. 8 shows the $\delta^{13}C_{DIC}$ and [DIC] conservative mixing lines plotted against salinity during all three seasons. We did not sample freshwater end member for the Mangalore region, hence mixing curve approximation for this region was not applied.

The deviations from the conservative mixing values of both DIC and $\delta^{13}C_{DIC}$ during the premonsoon and monsoon show the dominance of respiration/OM degradation over primary productivity. Although the summer monsoon coincides with the peak of the Arabian Sea primary production, the results show the dominance of mineralization to drive the Arabian Sea as a source of CO_2 to the atmosphere, which agrees very well with our observations. During the postmonsoon, the measured values of DIC and $\delta^{13}C_{DIC}$ were found to be close to conservative mixing lines with some exceptions.

5. Conclusions

Understanding different aspects of C dynamics in the Cochin estuary and the coastal Arabian Sea provide better insight to the flux of atmospheric CO_2 as well as terrestrial OM loading through estuaries. The present study used isotopic composition of C in dissolved inorganic

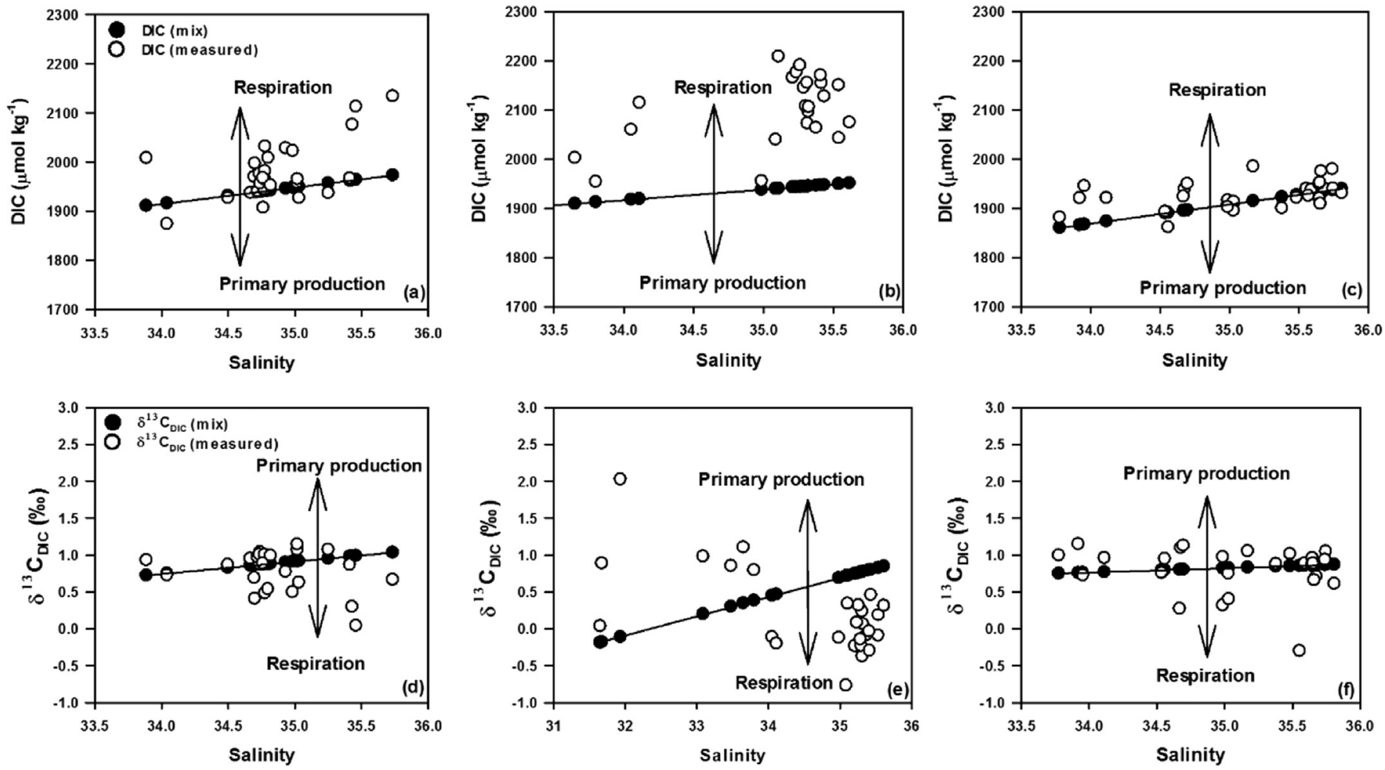

Fig. 8. Plots of DIC (upper panel) and $\delta^{13}C_{DIC}$ (lower panel) conservative (filled circle) and measured (open circle) values against salinity in the shelf waters of Cochin during premonsoon (a, d), monsoon (b, e), and postmonsoon (c, f). The arrows indicate the influence of primary productivity and OM degradation on the isotopic composition and concentration of DIC.

fractions to constrain the processes and sources of DIC in a complex estuarine-coastal coupled system. The isotopically constrained conservative mixing model suggests CO_2 degassing and freshwater mixing as dominant processes controlling C dynamics in the Cochin estuary during premonsoon and monsoon. However, during postmonsoon, the only sampling period characterized with dry and high tide phase, showed the presence of calcite precipitation in the regions with high salinity. Lower than model predicted $\delta^{13}C_{DIC}$ in the coastal waters and conservative mixing model suggest that the C dynamics in the coastal Arabian Sea is largely governed by respiration/OM degradation rather than primary production. This work also emphasizes the need for more detailed study vis-à-vis $\delta^{13}C_{DIC}$ with better constraints on end-members across the salinity gradient.

Acknowledgments

We thank Secretary, Ministry of Earth Sciences (MoES), Govt. of India and Director, Centre for Marine Living Resources and Ecology, Cochin, India for their support to this study. This study was funded by MoES (SIBER) and Indian Space Research Organization – Geosphere Biosphere Program, Department of Space, Govt. of India(ISRO-IGBP). This publication is CMLRE contribution number 87.

References

Abril, G., Etcheber, H., Delille, B., Frankignoulle, M., Borges, A.V., 2003. Carbonate dissolution in the turbid and eutrophic Loire estuary. Mar. Ecol. Prog. Ser. 259, 129–138.

Alling, V., Porcelli, D., Mörth, C.M., Anderson, L.G., Sanchez-Garcia, L., Gustafsson, Ö., Anderson, P.S., Humborg, C., 2012. Degradation of terrestrial organic carbon, primary production and out-gassing of CO_2 in the Laptev and East Siberian Seas as inferred from $\delta^{13}C$ values of DIC. Geochim. Cosmochim. Acta 95, 143–159.

Bhavya, P.S., Kumar, S., Gupta, G.V.M., Sudheesh, V., Sudharma, K.V., 2016a. Carbon isotopic composition of suspended particulate matter and dissolved inorganic carbon in the Cochin estuary during post-monsoon. Curr. Sci. http://dx.doi.org/10.18520/cs/v110/i8/1539-1543.

Bhavya, P.S., Kumar, S., Gupta, G.V.M., Sudheesh, V., Sudharma, K.V., Varrier, D.S., Dhanya, K.R., Saravanane, N., 2016b. Nitrogen uptake dynamics in a tropical eutrophic estuary (Cochin estuary) and adjacent coastal regions during pre-monsoon. Estuar. Coast. http://dx.doi.org/10.1007/s12237-015-9982-y.

Bhavya, P.S., Kumar, S., Gupta, G.V.M., Sudheesh, V., 2017. Carbon uptake rates in the Cochin estuary and adjoining coastal Arabian Sea. Estuar. Coast 40, 447–456. http://dx.doi.org/10.1007/s12237-016-0147-4.

Bouillon, S., Frankignoulle, M., Dehairs, F., Velimirov, B., Eiler, A., Etcheber, H., Abril, G., Borges, A.V., 2003. Inorganic and organic carbon biogeochemistry in the Gautami Godavari estuary (Andhra Pradesh, India) during pre-monsoon: the local impact of extensive mangrove forests. Glob. Biogeochem. Cycles 17 (4), 1114. http://dx.doi.org/10.1029/2002GB00202.

Broecker, W.S., Peng, T.H., 1993. Evaluation of the ^{13}C constraint on the uptake of fossil fuel CO_2 by the ocean. Glob. Biogeochem. Cycles 7, 619–626.

Degens, E.T., Deuser, W.G., Haedrlch, R.L., 1969. Molecular structure and composition offish otoliths. Mar. Biol. 2, 105–113.

de Jonge, V.N., Villerius, L.A., 1989. Possible role of carbonate dissolution in estuarine phosphate dynamics. Limnol. Oceanogr. 34, 332–340.

Dickson, A.G., Goyet, C., 1998. Handbook of Methods for the Analysis of the Various Parameters of the Carbon Dioxide System in Seawater, Version 2, Rep. ORNL/CDIAC-74. Dep. of Energy, Oak Ridge, Tennessee.

Erlenkeuser, H., Cordt, H.H., Simstich, J., Bauch, D., Spielhagen, R.F., 2003. DIC stable carbon isotope pattern in the surface waters of the southern Kara Sea, September 2000. In: Stein, R., Fahl, K., Fu¨ tterer, D.K., Galimov, E.M., Stepanets, O.V. (Eds.), Siberian River Run-off in the Kara Sea. Chemical Oceanography and the Marine Carbon Cycle. Elsevier Science, Amsterdam, pp. 281–307.

Frankignoulle, M., Borges, A.V., 2001. Direct and indirect pCO_2 measurements in a wide range of pCO_2 and salinity values. Aquat. Geochem. 7, 267–273.

Ghosh, P., Chakrabarti, R., Bhattacharya, S.K., 2013. Short- and long-term temporal variations in salinity and the oxygen, carbon and hydrogen isotopic compositions of the Hooghly Estuary water, India. Chem. Geol. 335, 118–127.

Grasshoff, K., Ehrhardt, M., Kremling, K., 1999. Methods of Sea Water Analysis, 3rd edn. VCH Publishers, Wainheins.

Gupta, G.V.M., Sarma, V.V.S.S., Robin, R.S., Raman, A.V., Jai Kumar, M., Rakesh, M., Subramanian, B.R., 2008. Influence of net ecosystem metabolism in transferring riverine organic carbon to atmospheric CO_2 in a tropical coastal lagoon (Chilka Lake, India). Biogeochemistry 87, 265–285.

Gupta, G.V.M., Thottathil, S.D., Balachandran, K.K., Madhu, N.V., Madeswaran, P., Nair, S., 2009. CO_2 supersaturation and net heterotrophy in a tropical estuary (Cochin, India): influence of anthropogenic effect. Ecosystems 12 (7), 1145–1157.

Gupta, G.V.M., Sudheesh, V., Sudharma, K.V., Saravanane, N., Dhanya, V., Dhanya, K.R., Lakshmi, G., Sudhakar, M., Naqvi, S.W.A., 2016. Evolution to decay of upwelling and associated biogeochemistry over the southeastern Arabian Sea shelf. J. Geophys. Res. Biogeosci. 121. http://dx.doi.org/10.1002/2015JG003163.

Keir, R.S., 1988. On the late Pleistocene ocean geochemistry and circulation. Paleoceanography 3, 413–445.

Krishna, M.S., Prasad, M.H.K., Rao, D.B., Viswanadham, R., Sarma, V.V.S.S., Reddy,

N.P.C., 2016. Export of dissolved inorganic nutrients to the northern Indian Ocean from the Indian monsoonal rivers during discharge period. Geochim. Cosmochim. Acta 172, 430–443.
Lewis, E., Wallace, D., Allison, L.J., 1998. Program Developed for CO_2 System Calculations. Carbon Dioxide Information Analysis Center, Oak Ridge National Laboratory, U. S. Department of Energy, Oak Ridge, Tennessee, pp. 38.
Madhupratap, M., 1987. Status and strategy of zooplankton of tropical Indian estuaries: a review. Bull. Plankton Soc. Jpn. 34, 65–81.
Martin, G.D., Jyothibabu, R., Madhu, N.V., Balachandran, K.K., Nair, Maheswari, Muraleedharan, K.R., Arun, P.K., Haridevi, C.K., Revichandran, C., 2013. Impact of eutrophication on the occurrence of *Trichodesmium* in the Cochin backwaters, the largest estuary along the west coast of India. Environ. Monit. Assess. 185 (2), 1237–1253.
Millero, F.J., Graham, T.B., Huang, F., Bustos-Serrano, H., Pierrot, D., 2006. Dissociation constants of carbonic acid in seawater as a function of salinity and temperature. Mar. Chem. 100 (1-2), 80–94. http://dx.doi.org/10.1016/j.marchem.2005.12.001.
Mook, W.G., 1970. Stable carbon and oxygen isotopes of natural waters in the Netherlands. Isot. Hydrol. 163–190.
Mook, W., Tan, F., 1991. SCOPE 42-Biogeochemistry of Major World Rivers.
Naqvi, S.W.A., Naik, H., Jayakumar, A., Pratihary, A.K., Narvekar, G., Kurian, S., Agnihotri, R., Shailaja, M.S., Narvekar, P., 2009. Seasonal anoxia over the western continental shelf. Indian Ocean Biogeochemical Processes and Ecological variability. Geophys. Monogr. Ser. 185, 333–345.
Oana, S., Deevey, E.S., 1960. Carbon 13 in lake waters and its possible bearing on paleolimnology. Am. J. Sci. 258, 253–272.
Quay, P.D., Tilbrook, B., Wong, C.S., 1992. Oceanic uptake of fossil fuel CO_2: carbon-13 evidence. Science 256, 74–79.
Quay, P., Sonnerup, R., Westby, T., Stutsman, J., McNichol, A., 2003. Changes in the $^{13}C/^{12}C$ of dissolved inorganic carbon in the ocean as a tracer of anthropogenic CO_2 uptake. Glob. Biogeochem. Cycles 17 (1), 1004. http://dx.doi.org/10.1029/2001GB001817.
Racapé, V., Lo Monaco, C., Metzl, N., Pierre, C., 2010. Summer and winter distribution of $\delta^{13}C_{DIC}$ in surface waters of the South Indian Ocean (20–60° S). Tellus B 62 (5), 660–673. http://dx.doi.org/10.1111/j.1600-0889.2010.00504.
Samanta, S., Dalai, T.K., Pattanaik, J.K., Rai, S.K., Mazumdar, A., 2015. Dissolved inorganic carbon (DIC) and its $\delta^{13}C$ in the Ganga (Hooghly) River estuary, India: evidence of DIC generation via organic carbon degradation and carbonate dissolution. Geochim. Cosmochim. Acta 165, 226–248.
Sarma, V.V.S.S., 2003. Monthly variability in surface pCO_2 and net air-sea CO_2 flux in the Arabian Sea. J. Geophys. Res. Oceans. http://dx.doi.org/10.1029/2001JC001062.
Sarma, V.V.S.S., Kumar, N.A., Prasad, V.R., et al., 2011. High CO_2 emissions from the tropical Godavari estuary (India) associated with monsoon river discharges. Geophys Res. Lett. 38, L08601. http://dx.doi.org/10.1029/2011GL046928.
Sarma, V.V.S.S., Viswanadham, R., Rao, G.D., Prasad, V.R., Kumar, B.S.K., Naidu, S.A., Murty, T.V.R., 2012. Carbon dioxide emissions from Indian monsoonal estuaries. Geophys. Res. Lett. 39 (3).
Thottathil, Shoji D., Balachandaran, K.K., Gupta, G.V.M., Madhu, N.V., Nair, Shanta, 2008. Influence of allochthonous input on autotrophic-heterotrophic switch-over in a shallow tropical ecosystem (Cochin Estuary), India. Estuar. Coast. Shelf Sci. 78, 551–562. http://dx.doi.org/10.1016/j.ecss.2008.01.018.
Sonnerup, R.E., Quay, P.D., McNichol, A.P., 2000. The Indian Ocean ^{13}C Suess effect. Glob. Biogeochem. Cycles 14, 903–916.
Srinivas, K., Revichandran, C., Maheswaran, P.A., Mohammed Ashraf, T.T., Nuncio, M., 2003. Propagation of tides in the Cochin estuarine system, southwest coast of India. Indian J. Geomar. Sci. 32 (14e24).
Sudheesh, V., Gupta, G.V.M., Sudharma, K.V., Naik, H., Shenoy, D.M., Sudhakar, M., Naqvi, S.W.A., 2016. Upwelling intensity modulates N_2O concentrations over the western Indian shelf. J. Geophys. Res.-Oceans 121, 8551–8565. http://dx.doi.org/10.1002/2016.JC012166.
Takahashi, T., Sutherland, S.C., Wanninkhof, R., Sweeney, C., Feely, R.A., Chipman, D.W., De Baar, H.J., 2009. Climatological mean and decadal change in surface ocean pCO_2, and net sea–air CO_2 flux over the global oceans. Deep-Sea Res. II: Top. Stud. Oceanogr. 56 (8), 554–577.
Valsala, V., Maksyutov, S., 2010. Simulation and assimilation of global ocean pCO_2 and air–sea CO_2 fluxes using ship observations of surface ocean pCO_2 in a simplified biogeochemical offline model. Tellus B 62 (5), 821–840.